

## Enhancing the Energy Content of Melawan Coal through $H_2SO_4$ and $NaOH$ Demineralization

Aliyu Buba Ngulde<sup>1,2\*</sup>, Wan Azlina Wan Ab Karim Ghani<sup>3\*\*</sup>, Nazmi Mat Nawi<sup>1,4</sup>, Umer Rashid<sup>5,6,7</sup>, and Kiman Silas<sup>2</sup>

<sup>1</sup>Institute of Plantation Studies, Universiti Putra Malaysia (UPM), Serdang, Selangor 43400, Malaysia

<sup>2</sup>Department of Chemical Engineering, Faculty of Engineering, University of Maiduguri, PMB 1069, Maiduguri, Borno State, Nigeria

<sup>3</sup>Sustainable Process Engineering Research Center (SPERC), Department of Chemical and Environmental Engineering, Faculty of Engineering, Universiti Putra Malaysia, Serdang, Selangor 43400, Malaysia

<sup>4</sup>Department of Biological and Agricultural Engineering, Universiti Putra Malaysia, Serdang, Selangor 43400, Malaysia

<sup>5</sup>Institute of Nanoscience and Nanotechnology (ION2), Universiti Putra Malaysia, Universiti Putra Malaysia, Serdang, Selangor 43400, Malaysia

<sup>6</sup>Center of Excellence in Catalysis for Bioenergy and Renewable Chemicals (CBRC), Faculty of Science, Chulalongkorn University, Pathumwan, Bangkok 10330, Thailand

<sup>7</sup>Department of Chemical Technology, Faculty of Science, Chulalongkorn University, Pathumwan, Bangkok 10330, Thailand

\* Corresponding author:

email: abngulde@unimaid.edu.ng\*;  
wanazlina@upm.edu.my\*\*

Received: September 18, 2024

Accepted: April 12, 2025

DOI: 10.22146/ijc.100059

**Abstract:** The objective of this study was to compare the calorific values, proximate analysis, ultimate analysis, SEM-EDX, XRF, FTIR spectroscopy, and TGA of the control feedstock and coal samples treated with different acid-alkali formulations. We also evaluated the effectiveness of the acid and alkali treatments, individually and in combination, on the structural and chemical properties of Melawan coal. The TGA results indicated that all treated coal samples showed reduced weight loss compared to raw coal, indicating the removal of minerals and volatile components owing to the treatment processes. Based on the DTG curve, the combination treatment (acid followed by base) somewhat stabilizes the coal, leading to a broader and less intense peak. EDS analysis revealed that both  $H_2SO_4$  and  $NaOH$  treatments, individually and in combination, significantly altered the elemental composition of the coal. According to FTIR analysis, the presence of carbonyl groups can affect the performance of coal in processes such as gasification, pyrolysis, or combustion, making it a key functional group of interest for evaluating post-treatment coal properties. The removal of mineral impurities can lead to a higher calorific value, making coal more suitable for energy generation applications.

**Keywords:** coal composition; demineralization; Melawan coal; coal power plant; coal properties

### ■ INTRODUCTION

There has been a significant increase in the world's energy demand due to population growth and economic development [1]. Power and heat generation are two routes utilizing various energy sources [2]. The world's power generation is primarily driven by coal, producing

approximately 38% of our electricity supply, and its use is expected to remain stable in the short term while developing countries are at the center of the rise in coal demand [3]. However, coal is at the center stage of the energy value chain as a sedimentary rock composed of non-combustible minerals from ash, fluids, and organic

carbonaceous matter (macerals) with vast applications in electricity generation and the kiln of cement plants for heat generation [4]. As a combustible fossil fuel, coal contains carbon, oxygen, hydrogen, sulfur, nitrogen, and trace amounts of various other elements [5]. It also has a complex structure with a high carbon content and calorific value, making it suitable for use as a main energy and chemical resource [2]. However, stabilizing and ensuring the energy sector's safety is of great significance [6]. Coal ash combustion's primary generates solid waste products so solid waste management is a substantial challenge for power plants and local authorities [7].

The coal demineralization is a process aimed at reducing its inorganic mineral content, which has various implications for its properties and applications. Studies have shown that demineralization can lead to changes in the pore distribution and surface area of coal, affecting its porosity and reactivity [8]. This process is particularly relevant for coals with low to moderate ash content, where demineralization is proposed to enhance its performance in applications such as solid oxide fuel cells [9]. By removing most of the inorganic species from coal, demineralization allows for a more focused study of the organic components and their behavior, such as in low-temperature oxidation studies [10]. Chemical demineralization procedures have been developed to alter the structure and reactivity of coal, significantly influencing its combustion characteristics [11]. Demineralized coal has been observed to produce different gas products than untreated coal, with variations in the formation of HCN and NH<sub>3</sub> [12]. Additionally, demineralization can affect the permeability of coal by reducing mineral occlusions in cleats, which are known to hinder permeability [13].

Various methods, including inorganic and organic acids, alkalis, and oxidants, have been employed for the demineralization and desulfurization of coal to reduce the ash and sulfur contents [14]. The beneficiation potential of demineralization has been explored for low-grade coals, showing promising results in reducing the ash content to meet the requirements for coal-generated electricity [15]. Furthermore, demineralization has been linked to modifications in the coal structure, affecting its

physical and chemical properties [16]. Literature reviews have reported that the coal demineralization positively impacts the use of chemicals. In contrast, the demineralization of coal plays a crucial role in altering its composition and properties, with implications for its reactivity, combustion behavior, and industrial applications.

This study aims to investigate the effects of acid-alkali sequential demineralization on the energy content and ash reduction of Melawan coal. This study systematically analyzes calorific value changes, proximate and ultimate composition, morphological structure, and elemental composition to evaluate the effectiveness of various acid-alkali formulations in removing deleterious minerals. The findings introduce a novel synergistic treatment strategy that optimized coal energy content and carbon composition while significantly reducing mineral impurities. These findings optimize coal beneficiation techniques for improved fuel quality and reduced environmental impact.

## ■ EXPERIMENTAL SECTION

### Materials

The coal samples were collected from Melawan in Indonesia. The coals were then crushed in a ball mill and sieved to -16+100 British standard sieve (BSS) mesh-size particles for conducting the experiments. Before the actual start of the experiment, the coal sample was characterized by using standard proximate (ASTM D3172-13) and ultimate (ASTM D3176-15) analysis methods while the calorific value of feedstocks was detected using the oxygen bomb calorimeter (IKA C 2000). The chemical reagents used in the present work is the commercially available sulfuric acid (H<sub>2</sub>SO<sub>4</sub> 98% concentration by wt.%) and sodium hydroxide (NaOH) pellets. A ceramic hotplate magnetic stirrer, a 1 L reaction flask with distilled water, and an oven were also utilized in this experiment.

### Instrumentation

Several instruments have been used in the experimental process, they include a ball mill, sieve shaker, 1 L reaction flask, ceramic hot plate, magnetic

stirrer, and oven. To carry out an investigation on the morphology of the feedstock scanning electron microscope (SEM) was utilized, a bomb calorimeter was also used to evaluate the energy content of the fuel, energy-dispersive X-ray fluorescence spectroscopy (EDS-XRF) machine was utilized as well as The Fourier transform Infrared spectroscopy (FTIR).

### Procedure

#### Demineralization

The demineralization process was conducted in a 1 L reaction flask placed on a ceramic hotplate magnetic stirrer. Initially, 50 g of coal was added to a reaction flask containing 20%  $\text{H}_2\text{SO}_4$  solution and stirred continuously at 600–900 rpm for 2 h at temperatures ranging from 65–100 °C. After filtration, the slurry was dried in an oven at 105 °C for 24 h, and the resulting  $\text{H}_2\text{SO}_4$ -treated coal was stored in closed containers. In the subsequent experiments, 50 g of coal was treated with NaOH solutions of varying concentrations (50, 100, and 150 g/L NaOH), following the same procedure. In the last phase of this experiment, each NaOH-treated coals sample underwent an additional washing step with 20%  $\text{H}_2\text{SO}_4$  to further enhance demineralization. This implies that 20%  $\text{H}_2\text{SO}_4$  Coal, 50 g/L NaOH Coal, 100 g/L NaOH Coal, 150 g/L NaOH Coal, 20%  $\text{H}_2\text{SO}_4$  50 g/L NaOH Coal, 20%  $\text{H}_2\text{SO}_4$  100 g/L NaOH Coal, and 20%  $\text{H}_2\text{SO}_4$  150 g/L NaOH Coal. Fig. 1 depicts the experimental and treatment sequence.

#### Proximate and ultimate analysis

The proximate analysis was investigated based on ASTM Standard D3173, the ultimate analysis, and was

deduced based on ASTM standard D3176-15 (LECO CHN analyzer), while the coal calorific value was determined using a bomb calorimeter (IKA C2000) in accordance with the previous study [3].

### Characterization

Thermogravimetric analysis (TGA) of sawdust was done using a thermogravimetric analyzer (Mettler Toledo equipment) at a rate of 10 °C/min up to 1000 °C under constant  $\text{N}_2$  flow rates of 50 mL/min. SEM analysis was conducted using JEOLJSM IT 300 LV (Germany) to characterize the coal samples morphology. The elemental analysis is carried out using an EDS-XRF analytical system (Model-XR300.50KV). FTIR analysis was carried out using Perkin Elmer RX to record the spectra in the range of 3800–400  $\text{cm}^{-1}$ .

## RESULTS AND DISCUSSION

#### Proximate and Ultimate Analysis

The proximate and ultimate analysis data, along with the calorific values (CV) of the raw Melawan coal and its demineralized forms, are summarized in Table 1. The mineralization process involved initial treatment with 50 wt.%  $\text{H}_2\text{SO}_4$ , followed by NaOH treatments at concentrations of 50, 100, and 150 g/L. A subsequent leaching step with 20 wt.% of  $\text{H}_2\text{SO}_4$  was applied in each experimental run, yielding 20%  $\text{H}_2\text{SO}_4$  50 g/L NaOH Coal, 20%  $\text{H}_2\text{SO}_4$  100 g/L NaOH Coal, and 20%  $\text{H}_2\text{SO}_4$  150 g/L NaOH Coal. The CVs of all eight feedstocks were measured using an oxygen bomb calorimeter. Notably, treatment with 50 wt.% of  $\text{H}_2\text{SO}_4$  alone increased the CV from 21.85 MJ/kg in the raw coal (RC)

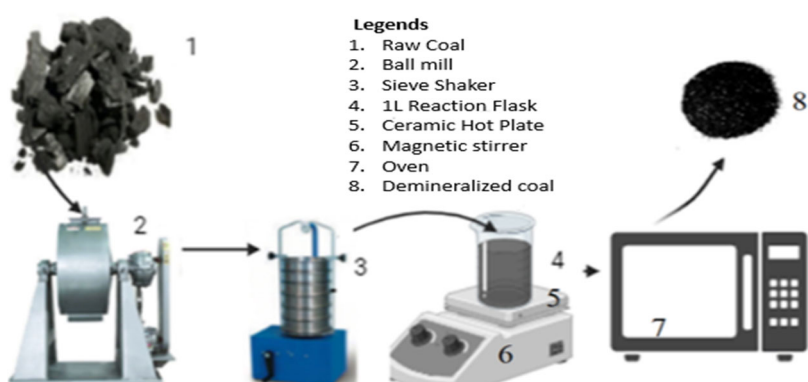


**Fig 1.** Experimental setup of Melawan coal demineralization using NaOH and  $\text{H}_2\text{SO}_4$

**Table 1.** Proximate, ultimate analysis, and calorific values of raw and demineralized coal

Sample	CV	C	H	N	S	O	H/C	O/C	MC	VM	FC	AC
Raw Coal (Melawan SB)	21.85	54.38	5.12	1.36	0.22	38.92	0.09	0.72	13.71	52.05	33.40	0.85
$\text{H}_2\text{SO}_4$ Coal	23.08	58.64	5.58	1.77	0.60	33.41	0.10	0.57	11.64	44.84	32.20	11.32
50 g/L NaOH Coal	15.61	50.20	5.05	1.30	0.18	43.27	0.10	0.86	13.91	44.98	31.90	9.21
100 g/L NaOH Coal	18.10	50.92	5.09	1.31	0.20	42.48	0.10	0.83	13.83	44.95	31.92	9.30
150 g/L NaOH	19.47	51.05	5.58	1.58	0.13	41.66	0.11	0.82	13.27	44.90	26.66	15.19
20% $\text{H}_2\text{SO}_4$ 50g/L NaOH Coal	19.40	51.01	5.57	1.56	0.13	41.73	0.11	0.81	13.30	44.91	31.95	9.84
20% $\text{H}_2\text{SO}_4$ 100g/L NaOH Coal	21.40	54.20	5.20	1.59	0.20	38.81	0.10	0.72	11.95	44.30	32.00	11.75
20% $\text{H}_2\text{SO}_4$ 150g/L NaOH Coal	22.36	59.02	5.63	1.70	0.82	32.83	0.10	0.57	11.42	43.12	32.08	13.38

to 23.08 MJ/kg. Additionally, elemental carbon content rose from 54.38 to 58.64 wt.%, indicating a more stable solid fuel compared to the control sample. A reduction in oxygen content was also observed, consistent with reported finding [17].

During alkali treatment with NaOH at varying concentrations, a significant drop in the energy content was observed, reaching 15.61 MJ/kg in 50 g/L NaOH-treated coal. However, energy content steadily increased with higher alkali concentrations, reaching 19.47 MJ/kg in 150 g/L NaOH-treated Coal, though still below the control feedstock. An increase in the carbon content with increasing alkali concentrations was observed, as the oxygen content also moved towards the control with increased alkali concentrations [4]. Subsequent leaching with 20%  $\text{H}_2\text{SO}_4$  significantly improved the energy compared to alkali treatment alone. The calorific value increased from 15.61 MJ/kg observed in 50 g/L NaOH-treated Coal to 19.40 MJ/kg in 20%  $\text{H}_2\text{SO}_4$  50 g/L NaOH-treated coal. Similar trends were noted with increasing alkali concentrations, culminating in a heating value of 22.36 MJ/kg in 20%  $\text{H}_2\text{SO}_4$  150 g/L NaOH-treated Coal. Additionally, elemental carbon content increased with acid leaching at each alkali concentration, accompanied by a corresponding decrease in oxygen content [5].

### TGA Analysis

Fig. 2 presents TGA curves, which show the influence of temperature on the weight percentages of various coal samples. The samples included RC, coal treated with  $\text{H}_2\text{SO}_4$ , coal treated with 20%  $\text{H}_2\text{SO}_4$  followed by 150 g/L NaOH, and coal treated with 150 g/L NaOH. The TGA curve of RC showed a gradual decrease in decrease in

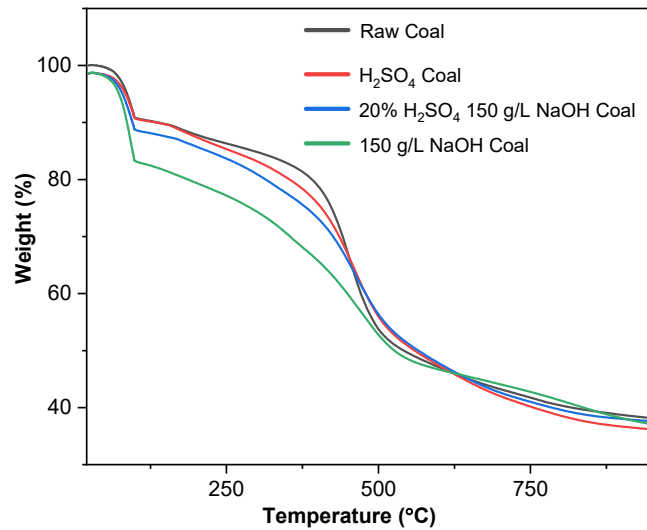


**Fig 2.** Influence of temperature change on percent weight

weight as the temperature increased. The initial weight loss (up to approximately 100 °C) can be attributed to moisture loss. The subsequent weight loss from 200 to 600 °C is likely due to the decomposition of volatile organic compounds and the combustion of fixed carbon. Above 600 °C, the weight loss continued but at a slower rate, indicating the combustion of more resistant carbon structures and the remaining inorganic components.

For coal treated with  $\text{H}_2\text{SO}_4$ , the overall weight loss appeared slightly lower than that of RC. The initial moisture loss region was similar to that of the RC. The red curve indicates that sulfuric acid treatment removed some mineral content, which resulted in a slightly different thermal degradation pattern. The weight loss between 200 and 600 °C was more gradual than that of RC, suggesting the removal of some volatile components or a change in the structure of the coal due to acid treatment. Coal

treated with 20%  $H_2SO_4$  followed by 150 g/L NaOH showed a further reduction in weight loss compared with both RC and coal treated only with  $H_2SO_4$ . The initial region, up to 100 °C, still exhibited moisture loss. The blue curve suggests that this combination of treatments removed additional mineral content and possibly more volatile compounds. The thermal stability of this sample was higher, as indicated by the lower weight loss between 200 and 600 °C. Finally, for coal treated with 150 g/L NaOH, the TGA curve shows the most significant reduction in weight, particularly in the initial stages. The initial weight loss up to 100 °C due to moisture was pronounced. The subsequent weight loss pattern was distinctly different, indicating a significant removal of the mineral content and changes in the organic structure of the coal. The green curve suggests that NaOH treatment led to the most significant structural and compositional changes, resulting in different thermal degradation behavior.

Fig. 3 shows differential thermogravimetric (DTG) curves of the same coal samples. The DTG curves represent the rate of weight loss ( $dm/dt$ ) as a function of the temperature, detailing the decomposition of each sample. The DTG curve for RC showed a prominent peak of approximately 450 °C, indicating the maximum rate of weight loss owing to the combustion of volatile organic compounds and fixed carbon. A smaller peak or shoulder was observed at approximately 100–150 °C, corresponding to moisture loss. The broad peak indicates a complex mixture of components with varying thermal stability. The red curve for coal treated with  $H_2SO_4$  has a noticeable peak shift toward lower temperatures compared to RC, with a maximum rate of weight loss occurring around 400–450 °C. This shift suggests that sulfuric acid treatment makes coal more thermally reactive, possibly due to the removal of certain minerals and the breakdown of some organic structures [6].

For the coal treated with 20%  $H_2SO_4$  followed by 150 g/L NaOH, the treatment appeared to slightly stabilize the coal compared to sulfuric acid treatment alone, indicated by a less pronounced peak at the maximum weight loss rate. The blue curve shows a peak similar to that of coal treated with sulfuric acid alone but with a slightly higher maximum temperature of approximately

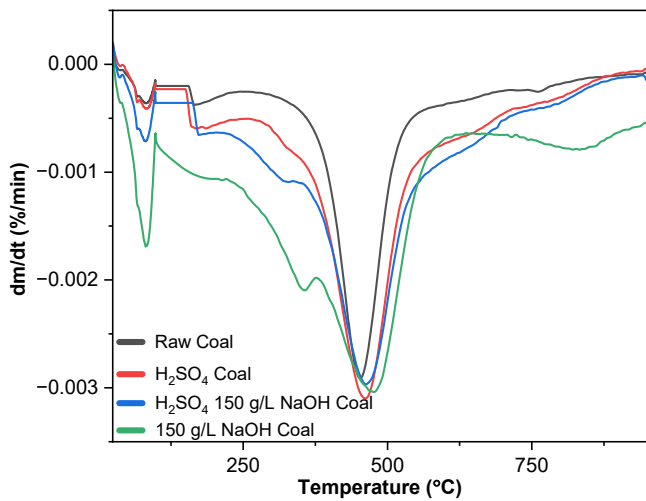


Fig 3. DTG curve of the coal sample

450 °C. In Fig. 3, the green curve shows a broader and more complex profile with multiple peaks. The primary peak around 450 °C was less sharp and lower in magnitude than those of the other treatments, indicating a slower rate of weight loss. There is an additional smaller peak at approximately 300 °C, possibly due to the breakdown of specific components altered by NaOH treatment. The overall DTG curve suggests that NaOH treatment significantly modifies the thermal degradation behavior of coal, making it more stable over a broader temperature range [18].

#### SEM Monograph

The surfaces of the RC particles appeared rough and uneven, indicating a complex and heterogeneous structure (Fig. 4). In addition, the image shows a range of particle sizes and shapes, with some particles appearing more angular and others rounded [19-20]. The rough surface suggests the presence of both macropores and micropores, which are typical in coal structures because of the heterogeneous composition of organic and inorganic materials. Bright spots on the surface could indicate the presence of mineral inclusions such as silicates, carbonates, or sulfides, which are commonly found in coal. The dark areas are likely organic-carbon-rich regions that form the bulk of the coal structure. The RC SEM image showed several pores and cavities, which are essential for understanding the adsorption properties of coal and its reactivity, particularly during combustion

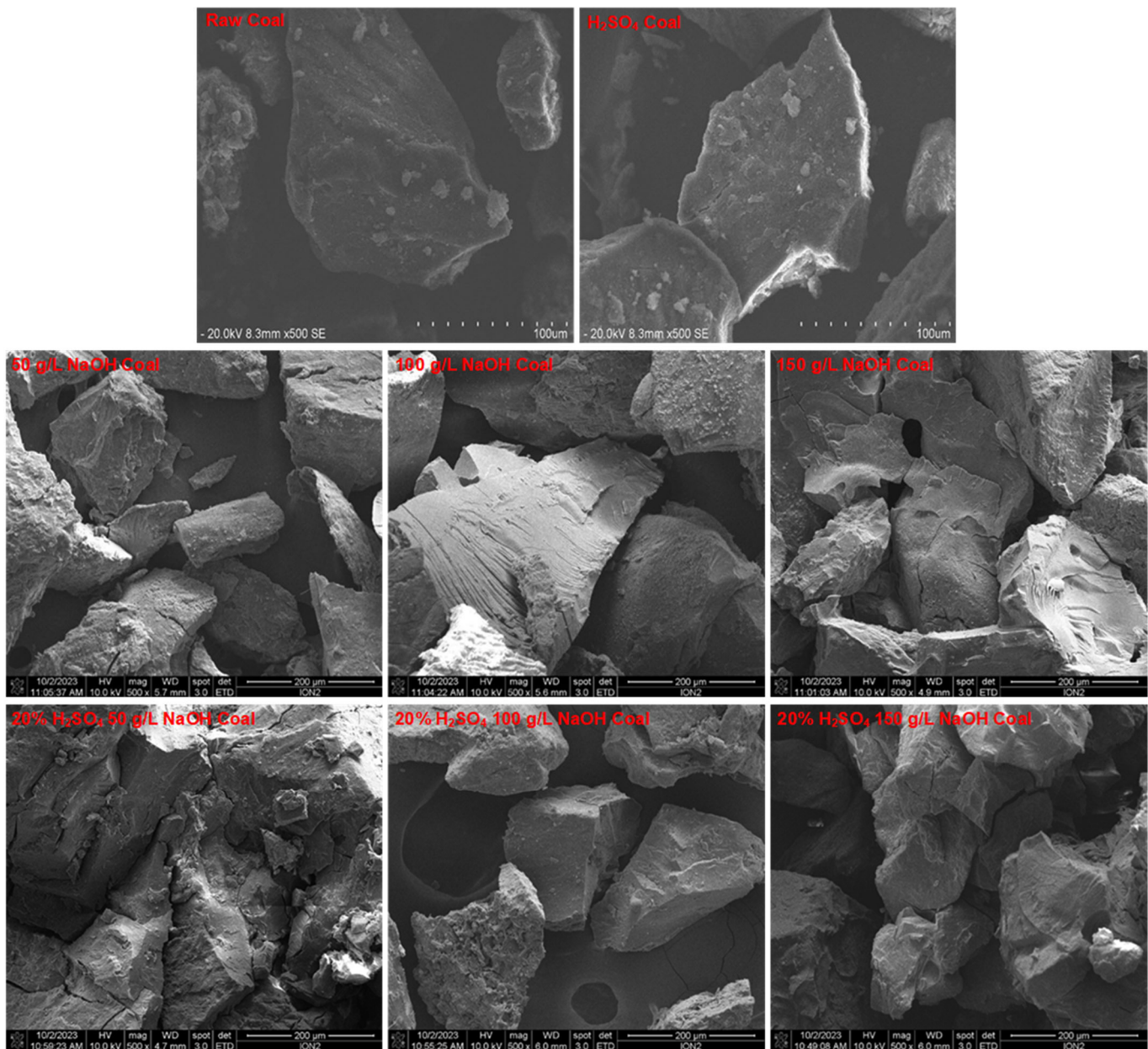


Fig 4. SEM micrograph of raw and demineralized coal

and gasification. There are visible fractures and cracks on the surface, which might be due to mechanical stress during sample preparation or inherent structural weaknesses in the coal, which can influence the mechanical strength of the coal and its behavior under thermal or pressure conditions.

The SEM images reveal several pores and cavities within the different types of coal samples. It also shows variations in surface texture among the different samples. The roughness and unevenness of the surface differed

based on the treatment applied, indicating varying degrees of mineral removal and structural changes. Differences in the particle size and shape were observed across the samples. Some samples exhibited more angular particles, whereas others showed rounded or irregular shapes, suggesting alterations in the coal structure due to the treatment conditions. Variances in the pore structure were observed, with some samples displaying a higher density of pores or larger pore sizes than others. The treatment processes likely influenced

the formation and distribution of pores in the coal samples. All the samples exhibited a heterogeneous composition, with a mix of organic and inorganic components visible in the SEM images. This heterogeneity is a typical characteristic of coal and is maintained under various treatment conditions.

### Elemental and Mineral Composition

The energy dispersive X-ray spectroscopy (EDS) analysis results (Table 2) show the elemental composition (in weight percentage) of RC and coal treated with various concentrations of NaOH and H<sub>2</sub>SO<sub>4</sub>. Table 2 shows that the RC is naturally high in carbon and oxygen, which are typical characteristics of coal. Upon treatment with H<sub>2</sub>SO<sub>4</sub>, there was a slight reduction in the carbon content and an increase in the oxygen content, suggesting oxidation or introduction of oxygen-containing functional groups. NaOH treatment resulted in variable changes: the carbon content decreased at lower NaOH concentrations but recovered at higher concentrations, while the oxygen content showed the opposite trend. The combined NaOH and H<sub>2</sub>SO<sub>4</sub> treatment yielded a higher carbon content compared to the single treatments, indicating effective impurity removal and stabilization of organic structures [21].

Additionally, RC contains impurities, such as aluminum, silicon, sulfur, calcium, and iron. However, H<sub>2</sub>SO<sub>4</sub> treatment generally reduces the aluminum and iron content while slightly increasing the silicon content, suggesting the selective removal of certain elements.

NaOH treatment eliminates aluminum, introduces significant sodium, and variably affects the presence of other elements, such as calcium and iron. The presence of sodium is due to the NaOH treatment. The combined NaOH and H<sub>2</sub>SO<sub>4</sub> treatment, as shown in Table 2, resulted in a higher sulfur content compared to the other treatments, possibly due to residual H<sub>2</sub>SO<sub>4</sub> or the formation of sulfate compounds [22].

Generally, H<sub>2</sub>SO<sub>4</sub> treatment increases oxygen content and reduces the number of metallic impurities. As shown in Table 2, NaOH treatment introduces sodium and significantly alters the carbon and oxygen content while variably impacting other elements. The combination of NaOH followed by H<sub>2</sub>SO<sub>4</sub> treatment was most effective in increasing the carbon content and reducing impurities, leading to a more refined coal structure [23]. This combination treatment stabilized the carbon content and removed most impurities, resulting in a unique elemental profile with an increased sulfur content. These chemical modifications are crucial for enhancing the performance of coal for various industrial applications. Furthermore, the composition of the mineral matter as a fraction of the oxide was analyzed using an XRF spectrometer (PANalytical Axios FAST XRF spectrometer, Japan). The results of this analysis are summarized in Table 3. The Fe<sub>2</sub>O<sub>3</sub>, Na<sub>2</sub>O, and SO<sub>3</sub> contents of the treated coal increased during the caustic treatment, but they were better dissolved in the acid-treated coal [24]. On the other hand, the SiO<sub>2</sub> and Al<sub>2</sub>O<sub>3</sub> contents increased in the combined treated coal,

**Table 2.** EDS analysis result

Element (wt.%)	Raw coal	H <sub>2</sub> SO <sub>4</sub>	NaOH concentration (g/L)			NaOH concentration (g/L) followed by 20% H <sub>2</sub> SO <sub>4</sub>		
			50	100	150	50	100	150
C	67.87	67.15	58.74	64.00	66.05	69.02	65.43	68.90
O	30.38	31.45	33.43	30.60	28.53	29.68	32.76	30.80
Al	0.54	0.28	-	-	-	-	-	-
Si	0.18	0.58	0.40	0.12	0.39	-	-	0.12
S	0.37	0.33	0.22	0.13	0.20	1.22	1.08	0.18
Ca	0.28	-	1.93	0.38	0.65	0.08	0.73	-
Fe	0.38	0.13	0.50	0.23	0.34	-	-	-
Ti	-	0.08	-	-	-	-	-	-
Na	-	-	4.69	4.54	3.66	-	-	-
Mg	-	-	0.09	-	0.20	-	-	-

**Table 3.** XRF detected ash composition of various coal samples

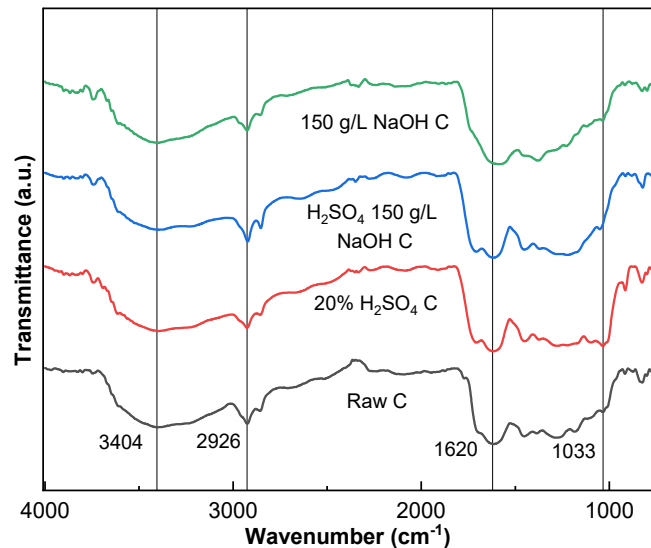
Coal type	Ash composition (%)								
	Fe <sub>2</sub> O <sub>3</sub>	CaO	SO <sub>3</sub>	SiO <sub>2</sub>	K <sub>2</sub> O	MnO	CuO	Er <sub>2</sub> O <sub>3</sub>	Cr <sub>2</sub> O <sub>3</sub>
Raw Coal	44.09	21.91	16.48	15.98	0.69	0.85	-	-	-
H <sub>2</sub> SO <sub>4</sub> Coal	34.24	2.57	37.24	22.82	1.44	-	-	1.23	0.46
150 g/L NaOH Coal	41.66	27.01	9.79	19.38	0.99	0.60	0.59	-	-
150 g/L NaOH with 20% H <sub>2</sub> SO <sub>4</sub> Coal	15.09	10.54	57.64	16.74	-	-	-	-	-

while they reduced to above 50% alone with caustic treatment by dissolution and formation of sodium silicate ( $\text{Na}_2\text{SiO}_3$ ) and sodium aluminate ( $\text{NaAlO}_2$ ) in the leaching process. Most of the quartz ( $\text{SiO}_2$ ) and alumina ( $\text{Al}_2\text{O}_3$ ) dissolved during caustic treatment. During the ash analysis, red-colored ash was found in the caustic-treated coal, which may be due to the presence of  $\text{Fe}_2\text{O}_3$  (hematite),  $\text{Na}_2\text{O}$  and other minerals, whereas white-colored ash was found due to the presence of a large amount of  $\text{SiO}_2$  and  $\text{Al}_2\text{O}_3$  in the combined treated coal [25].

### FTIR Spectrophotometry

In Fig. 5, which represents the RC FTIR, the functional groups indicated typically include various organic functional groups present in coal [26]. These may include, but are not limited to, aliphatic C–H, aromatic C=C, C=O, O–H, and C–O stretching. The FTIR spectrum helps identify the chemical bonds and functional groups present in the coal sample [20]. In Fig. 5, 50 wt.%  $\text{H}_2\text{SO}_4$  Coal, 150 g/L NaOH Coal, and 50 wt.%  $\text{H}_2\text{SO}_4$  150 g/L NaOH Coal FTIR spectrum exhibit peaks corresponding to specific functional groups in the coal sample. The values of these peaks can vary depending on the specific coal composition and treatment. Common peaks and their corresponding functional groups in the coal FTIR spectra include aliphatic C–H typically observed around 2800–3000  $\text{cm}^{-1}$ , aromatic C=C peaks around 1500–1600  $\text{cm}^{-1}$ , C=O peaks around 1700–1750  $\text{cm}^{-1}$ , O–H peaks can be seen around 3200–3600  $\text{cm}^{-1}$ , and C–O peaks around 1000–1300  $\text{cm}^{-1}$  [27].

The functional group that is particularly important in the FTIR analysis of coal samples is the C=O groups. This functional group is significant for several reasons related to the demineralization and treatment of coal using acids and alkalis. Carbonyl groups can influence the reactivity of coal during combustion. Changes in the C=O

**Fig 5.** Raw and demineralized Melawan coal FTIR

stretching peak intensity or position in the FTIR spectrum indicate alterations in the chemical structure of the coal, which may impact its combustion characteristics [28]. The presence or absence of carbonyl groups reflects the effectiveness of demineralization treatments ( $\text{H}_2\text{SO}_4$  and NaOH) on coal. Changes in the C=O stretching peak intensity or shape after treatment clearly explain the chemical modifications induced by acid and alkali processes [8]. The specific peak values corresponding to carbonyl groups vary depending on the coal composition and treatment processes. In Fig. 5, the peak value corresponding to the C=O group is observed around 1700–1750  $\text{cm}^{-1}$ .

### CONCLUSION

This study investigated the effects of acid-alkali ( $\text{H}_2\text{SO}_4$ , NaOH) sequential demineralization on the energy and ash content of Melawan coal, demonstrating its effectiveness in improving coal quality. The results confirmed that this treatment significantly enhanced the

calorific value while reducing deleterious mineral impurities, as evidenced by proximate and ultimate analysis, SEM-EDX, and XRF characterization. The synergistic effect of the acid-alkali process optimized the carbon composition while mitigating the adverse impact of alkali treatment alone. This novel approach offers a promising strategy for coal beneficiation, providing a more efficient method for enhancing coal's energy yield and reducing its environmental impact. Future studies could further optimize the demineralization process by exploring different reagent combinations and treatment conditions to maximize efficiency and industrial applicability.

## ■ ACKNOWLEDGMENTS

We acknowledged the profound support and contributions of the staff of the Universiti Putra Malaysia especially Encik Ismail of the Combustion Engineering Laboratory, Ali Rani of the Institute for Nanoscience and Nanotechnology, and the the OSS staff of PTDF. This research is funded by the Geran Inisiatif Putra Siswazah (GP-IPS), GP\_IPS/2023/9768900, and the Petroleum Technology Development Fund (PTDF) under PTDF/ED/OSS/PHD/EAB/1829/20 by 22PHD035.

## ■ CONFLICT OF INTEREST

The authors declare no conflict of interest.

## ■ AUTHOR CONTRIBUTIONS

Aliyu Buba Ngulde: Laboratory works and paper drafting and conceptualization. Wan Azlina Wan Ab Karim Ghani: Conceptualization, supervision and analysis. Nazmi Mat Nawi: Manuscript adjustments and final approval. Umer Rashid: Suitable paper selection and final approval. Kiman Silas: Reviews. All authors reviewed and agreed to the final version of this manuscript.

## ■ REFERENCES

- [1] Ngulde, A.B., Silas, K., Mohammed, H.D., Yaumi, A.L., Taura, U.H., and Mari, H.H., 2022, Conversion of biomass to adsorbent: A review, *Arid Zone J. Eng., Technol. Environ.*, 18 (1), 65–78.
- [2] Silas, K., Ngulde, A.B., and Mohammed, H.D., 2022, Utilization of date tree leaves biomass for the removal of heavy metals from water, *J. Eng. Res. Sci.*, 1 (4), 137–147.
- [3] Aich, S., Nandi, B.K., and Coal, H.A., 2025, Identification of combustion characteristics of high ash Indian coal, rice straw, rice straw char and their blends, *Process Saf. Environ. Prot.*, 193, 1243–1260.
- [4] Fikri, H.N., Sachsenhofer, R.F., Bechtel, A., and Gross, D., 2022, Organic geochemistry and petrography in Miocene coals in the Barito basin (Tutupan mine, Indonesia): Evidence for astronomic forcing in kerapah type peats, *Int. J. Coal Geol.*, 256, 103997.
- [5] Ngulde, A.B., Wan Binti Abdulkarim Ghani, W.A., Nawi, N.M., Rashid, U., and Kiman, S., 2025, Assessing bamboo culm of different ages as potential solid fuel for power generation, *Evergreen: Jt. J. Novel Carbon Resour. Sci. Green Asia Strategy*, 12 (1), 574–582.
- [6] Lin, Y., Qin, Y., Qiao, J., Li, G., and Zhang, H., 2022, Effect of coalification and maceration on pore differential development characteristics of high-volatile bituminous coal, *Fuel*, 318, 123634.
- [7] Gokce, Y., Yaglikci, S., Yagmur, E., Banford, A., and Aktas, Z., 2021, Adsorption behaviour of high performance activated carbon from demineralised low rank coal (Rawdon) for methylene blue and phenol, *J. Environ. Chem. Eng.*, 9 (2), 104819.
- [8] Zhang, G., Ranjith, P.G., Perera, M.S.A., Haque, A., Choi, X., and Sampath, K.S.M., 2018, Characterization of coal porosity and permeability evolution by demineralisation using image processing techniques: A micro-computed tomography study, *J. Nat. Gas Sci. Eng.*, 56, 384–396.
- [9] Zdeb, J., Howaniec, N., and Smoliński, A., 2023, Experimental study on combined valorization of bituminous coal derived fluidized bed fly ash and carbon dioxide from energy sector, *Energy*, 265, 126367.
- [10] Prasad, S.K., and Mangaraj, B.K., 2022, A multi-objective competitive-design framework for fuel procurement planning in coal-fired power plants for sustainable operations, *Energy Econ.*, 108, 105914.
- [11] Silas, K., Undiandeye, J., and Kefas, H.M., 2023, Demineralization and characterization of coal

deposit found in Maiganga, Akko Local Government, Gombe State, Nigeria, *Arid Zone J. Basic Appl. Res.*, 2 (1), 126–138.

[12] Usman, T., Abicho, S., Meshesha, D., and Adam, G., 2022, Froth flotation beneficiation and physiochemical characterization of coal from Achibo-Sombo-Dabaso area, southwestern Ethiopia, *Helijon*, 8 (11), e11313.

[13] Fan, C., Wang, B., Ai, H., Qi, Y., and Liu, Z., 2021, A comparative study on solidification/stabilization characteristics of coal fly ash-based geopolymers and Portland cement on heavy metals in MSWI fly ash, *J. Cleaner Prod.*, 319, 128790.

[14] Wiranata, D.Y., Yang, S.H., Akgul, C.M., Hsien, H.Y., and Nugraha, M.Z.P., Use of coal ash cement stabilized material as pavement base material: Laboratory characterization and field evaluation, *Constr. Build. Mater.*, 344, 128055.

[15] Okolo, G.N., Everson, R.C., H. Neomagus, H.W.J.P., Roberts, M.J., and Sakurovs, R., 2015, Comparing the porosity and surface areas of coal as measured by gas adsorption, mercury intrusion and SAXS techniques, *Fuel*, 141, 293–304.

[16] Kaklidis N., Kyriakou, V., Garagounis, I., Arenillas, A., Menéndez, J.A., Marnellos, G.E., and Konsolakis, M., 2014, Effect of carbon type on the performance of a direct or hybrid carbon solid oxide fuel cell, *RSC Adv.*, 4 (36), 18792–18800.

[17] Yip, K., Ng, E., Li, C.Z., Hayashi, J.I., and Wu, H., 2012, A mechanistic study on kinetic compensation effect during low-temperature oxidation of coal chars, *Proc. Combust. Inst.*, 33 (2), 1755–1762.

[18] Rubiera F., Arenillas, A., Pevida, C., García, R., Pis, J.J., Steel, K.M., and Patrick, J.W., 2002, Coal structure and reactivity changes induced by chemical demineralisation, *Fuel Process. Technol.*, 79 (3), 273–279.

[19] Hansson, K.M., Samuelsson, J., Åmand, L.E., and Tullin, C., 2003, The temperature's influence on the selectivity between HNCO and HCN from pyrolysis of 2,5-diketopiperazine and 2-pyridone, *Fuel*, 82 (18), 2163–2172.

[20] Turner, L.G., and Steel, K.M., 2016, A study into the effect of cleat demineralisation by hydrochloric acid on the permeability of coal, *J. Nat. Gas Sci. Eng.*, 36, 931–942.

[21] Dhawan, H., and Sharma, D.K., 2019, Advances in the chemical leaching (inorganico-leaching), bio-leaching and desulphurisation of coals, *Int. J. Coal Sci. Technol.*, 6 (2), 169–183.

[22] Nyoni, S., Bwalya, M., and Chimwani, N., 2020, Beneficiation potential of a low-grade coal from the Emalahleni (Witbank) coalfield, *Physicochem. Probl. Miner. Process.*, 56 (5), 849–859.

[23] Jiménez, A., Iglesias, M.J., Laggoun-Défarge, F., and Suárez-Ruiz, I., 1998, Study of physical and chemical properties of vitrinites. Inferences on depositional and coalification controls, *Chem. Geol.*, 150 (3-4), 197–221.

[24] Nakhaei, M., Grévain, D., Jensen, L.S., Glarborg, P., Dam-Johansen, K., and Wu, H., 2021, NO emission from cement calciners firing coal and petcoke: A CPFD study, *Appl. Energy Combust. Sci.*, 5, 100023.

[25] Harianingsih, H., Indriawan, A.N.D., Setiadi, R., Pangestu, I.S., Erliana, S.R., and Ubay, I.N., 2024, The improvement of modified rice straw fiber/polyvinyl alcohol thermoplastic polymer composite using cold plasma technology, *Indones. J. Chem.*, 24 (4), 1145–1155.

[26] Amri A., Ahmad, N., Wibiyan, S., Wijaya, A., Mardiyanto, M., Royani, I., Mohadi, R., Lesbani, A., 2024, Optimization of desulfurization of 4-methyldibenzothiophene and 4,6-dimethyldibenzothiophene using Mg/Al layered double hydroxide equipped with ZnO/TiO<sub>2</sub>, *Indones. J. Chem.*, 24 (4), 1011–1022.

[27] Al-Sarhan, A., Al-Massaedh, A.A., and Al-Momani, I.F., 2024, Assessment of heavy metal concentrations in roadside soils from Mafraq, Jordan, *Indones. J. Chem.*, 24 (4), 1071–1090.

[28] Sahoo, N., Kumar, A., and Samsher, S., 2022, Review on energy conservation and emission reduction approaches for cement industry, *Environ. Dev.*, 44, 100767.